Low Reynolds Number Modeling of Turbulent Flows With and Without Wall Transpiration

Ronald M. C. So* and Geun Jong Yoo†
Arizona State University, Tempe, Arizona

A full Reynolds-stress closure that is capable of describing the flow all the way to the wall is formulated. The closure is based on the conventional high Reynolds number form of the redistribution model, the inclusion of molecular diffusion, and a modified dissipation model to account for viscous effects near a wall. Two dissipation models are investigated along with two gradient diffusion and two redistribution models. Their respective effects on the calculated flow properties are assessed by comparing them with the data of fully developed turbulent flows and a developing pipe flow with wall transpiration. The near-wall behavior is very well predicted; however, the wall correction to the redistribution modeling is found to have little effect on the calculated results. The overall behavior of the fully developed turbulent flows is best described by a nonisotropic gradient diffusion model, a return-to-isotropy redistribution model, and a dissipation model that accounts for viscous behavior near a wall. This same closure also gives the best prediction of the axial pressure drop behavior along a pipe with a uniform wall suction. Furthermore, the near-wall behavior of such a flow is very well predicted by this closure.

I. Introduction

THE Reynolds-stress closure [closure schemes that solve the full set of Reynolds stress transport equations as well as models that solve the Reynolds shear stress and k equations alone (e.g., Refs. 1 and 2)] of turbulence applied to turbulent flow calculations was first examined by Hanjalic and Launder.[1] In their model, certain assumptions concerning the structure parameters $\overline{u_i u_i}/k$ (i not summed), where u_i is the ith component of the fluctuating velocity and $2k = \overline{u_i u_i}$ (summation over i) is the turbulence kinetic energy, were invoked to simplify the four Reynolds-stress transport equations for two-dimensional thin shear layers to two equations for turbulent shear stress and k. These were then solved with the mean flow equations and an equation governing the transport of ϵ, the dissipation rate of k. The closure was arrived at by assuming the flow Reynolds number to be very large and that $\overline{u_i u_i}/k$ = constant throughout the shear layer with the constants given by plane shear flow measurements. In view of these approximations, the boundary conditions cannot be applied at the wall. Rather, they were applied near the wall. In particular, the mean flow velocity was matched to the logarithmic law of the wall, the gradient of k was set equal to zero, the shear stress was determined from the mean momentum equation with the convection terms neglected, and ϵ was set equal to the turbulence generation rate. The model gave a good comparison with the measurements away from the wall for a wide variety of thin shear layers. However, detailed flow modeling near a wall remained unattainable.

In view of the initial success of the Reynolds-stress closure, later researchers[3-8] relaxed the assumption $\overline{u_i u_i}/k$ = constant throughout the shear layer and solved the full set of Reynolds-stress transport equations. However, the large-Reynolds-number assumptions were retained in the modeling of turbulent diffusion, redistribution, and viscous dissipation rate terms in the Reynolds-stress transport equations. Consequently, the boundary-layer flow very near the wall had to be handled in the same manner as that proposed by Hanjalic and Launder.[1] The boundary conditions for $\overline{u_i u_i}$ near a wall, however, required special attention. In general, either a slip condition for $\overline{u_i u_i}$ was imposed[6] or the Neuman boundary conditions were specified.[5] The amount of slip specified for $\overline{u_i u_i}$ depended to a great extent on the type of flow considered. As a result, the closure was problem-dependent and, in spite of the improvement, it still could not provide an accurate description of the flow very near the wall. This in turn means that the Reynolds-stress closure cannot be used to estimate the Reynolds number effects on turbulent flows, because in the immediate vicinity of a wall, the viscous effects have to be important.[4]

The logarithmic law of the wall assumption was generally applicable for a wide class of simple wall shear flows. However, it failed to provide a reasonably accurate estimate of the near-wall mean velocity in separating flows, relaminarizing flows, flows with wall transpiration, and complex wall shear flows.[9-12]. In order to remedy this unsatisfactory boundary condition, Hanjalic and Launder[2] applied the arguments of Jones and Launder[13] to modify their Reynolds-stress closure to account for the viscosity effects near a wall. In their new closure, they relaxed the assumption $\overline{u_i u_i}/k$ = constant. Instead, they assumed that $(3/4)(\overline{u_1^2} + \overline{u_2^2}) = k$ and $\overline{u_2^2} \simeq 4(\overline{u_1 u_2})^2/k$ based on the pipe and channel flow measurements of Laufer[14] and Eckelman.[15] This way the near-wall behavior of $\overline{u_2^2}/k$, i.e., $\overline{u_2^2}/k \to 0$ as $x_2 \to 0$, was satisfied. Their calculated mean velocity and shear stress results were in excellent agreement with the channel flow measurements of Patel and Head[16] and Eckelman[15] and the relaminarizing flow data of Jones and Launder.[10] In spite of these successes, a low Reynolds number Reynolds-stress closure, where all the transport equations for $\overline{u_i u_j}$ are solved rather than the equations for k and $\overline{u_1 u_2}$ alone, is still not available.

The primary objective of this paper is to formulate and validate such a model so that the calculations can be carried all the way to the wall and satisfy the boundary conditions at the wall for U_i, $\overline{u_i u_j}$, and ϵ. The calculated results from a number of closures are first compared with fully developed turbulent flow data at several Reynolds numbers and then compared with flows with wall transpiration where the wall-function approximation is known to be inadequate. Fully

Received Oct. 29, 1986; revision received March 19, 1987.

*Professor, Mechanical and Aerospace Engineering Department.
†Graduate Assistant, Mechanical and Aerospace Engineering Department.

developed turbulent flows are selected as the first test because the governing equations simplify to second-order, nonlinear ordinary differential equations. This simplification allows the various modeling assumptions to be assessed easily. Therefore, the models of Rotta[17] and Launder et al.[7] for redistributions are examined in detail together with a nonisotropic[2] and an isotropic[18] gradient diffusion model for turbulent diffusion. Once validated for simple wall shear flows, the closures are extended to calculate complex flows where the wall-function approximation is inadequate, and the flows are governed by an elliptic set of partial differential equations.

II. Low Reynolds Number Turbulence Model

For an incompressible flow, the transport equations for the Reynolds stresses $(\overline{u_i u_j})$ can be concisely expressed in Cartesian tensor as

$$\frac{D\overline{u_i u_j}}{Dt} = \frac{\partial}{\partial x_k}\left[-\overline{u_i u_j u_k} - \frac{p}{\rho}\left(\overline{\delta_{ik} u_j + \delta_{jk} u_i}\right) + \nu \frac{\partial \overline{u_i u_j}}{\partial x_k} \right] - \left[\overline{u_j u_k} \frac{\partial U_i}{\partial x_k} + \overline{u_i u_k} \frac{\partial U_j}{\partial x_k} \right] + \overline{\frac{p}{\rho}\left(\frac{\partial u_i}{\partial x_j} + \frac{\partial u_j}{\partial x_i} \right)} - 2\nu \overline{\frac{\partial u_i}{\partial x_k} \frac{\partial u_j}{\partial x_k}} \tag{1a}$$

or symbolically as

$$C_{ij} = D_{ij}^T + D_{ij}^v + P_{ij} + \Phi_{ij} - \epsilon_{ij} \tag{1b}$$

Here, lower and upper case u_i denote fluctuating and time-averaged velocity components respectively, p denotes fluctuating pressure, ρ and ν are the fluid density and kinematic viscosity respectively, and overbars imply the usual time averaging of the correlations in question.

The terms in Eq. (1), from left to right, can generally be interpreted as the convection, diffusion (turbulent and molecular), production, redistribution, and viscous dissipation of $\overline{u_i u_j}$, respectively. In the past, Eq. (1) was normally closed by assuming the flow Reynolds number to be very large. Consequently, the molecular diffusion was neglected, and the viscous dissipation was assumed to be isotropic and was so modeled.[19] Many models for turbulent diffusion and redistribution are proposed, and some of the more common models can be found in Refs. 1, 2, 5, 7, 17, 18, and 20. For near-wall flows, the conventional models are inadequate and have to be modified. Since the redistribution term has a zero trace for an incompressible flow, it acts to diminish the difference between the normal stress components.[21] Therefore, it neither produces nor destroys turbulence energy. In addition, ν does not appear explicitly in the equation for $\nabla^2 p$, obtained by taking the divergence of the equation for u_i. These facts suggest that, to the first order, any high Reynolds number model for the redistribution term can be adopted for near-wall flows. Specifically, the models of Rotta[17] and Launder et al.[7] with and without wall correction are considered. As for turbulent diffusion modeling, the conventional models are applicable. Specifically, the models of Hanjalic and Launder[2] and Daly and Harlow[18] are examined. Therefore, this leaves the viscous dissipation model to be considered and modified.

At the wall, $\overline{u_i u_j} = a_{ij} y^N + b_{ij} y^{N+1} + \cdots$ (see Ref. 4), where $N \geq 2$, $a_{ij}, b_{ij}, \cdots$ are constants to be determined, $y = R - r$, r is the normal coordinate measured from the symmetry plane, and R is the channel half-width or pipe radius. For fully developed pipe or channel flows, the substitution of this expansion into $D_{ij}^v = (\partial/\partial x_k)(\nu \partial \overline{u_i u_j}/\partial x_k)$ gives

$$D_{ij}^v = \frac{1}{r^J}\frac{\partial}{\partial r}\left(r^J \nu \frac{\partial \overline{u_i u_j}}{\partial r} \right) = (N-1) N a_{ij} \nu y^{N-2} + \left[N(N+1) b_{ij} \nu - \frac{J N a_{ij} \nu}{R - y} \right] y^{N-1} + O(y^N) \tag{2}$$

where $J = 0$ or 1 for channel or pipe flows, respectively. Therefore, for $N = 2$, all the terms on the right-hand side of Eq. (2), except the first term, vanish at $y = 0$, and this is true for all near-wall flows. This means that molecular diffusion is finite at the wall. Since the term D_{ij}^v does not need modeling and ν does not appear in other diffusion terms, additional terms are required in the modeling of the dissipation function $2\nu(\overline{\partial u_i/\partial x_k})(\overline{\partial u_j/\partial x_k})$ in order to balance the finite molecular diffusion at the wall.

The foregoing argument, therefore, suggests that the Kolmogorov[19] high Reynolds number model for the dissipation function should be modified to give

$$\epsilon_{ij} = 2\nu \overline{\frac{\partial u_i}{\partial x_k} \frac{\partial u_j}{\partial x_k}} = \frac{2}{3}\delta_{ij}\epsilon + \frac{2\nu \delta_{i1}\delta_{jm} \overline{u_1 u_m}}{x_2^2} \tag{3}$$

for low Reynolds number flows, where ϵ is the isotropic dissipation rate of the turbulent kinetic energy k and x_2 is measured normal from the wall. The dissipation model equation (3) is essentially a generalization of Chien's[22] proposed modification of the k equation for near-wall flows. As such, it represents a simple extension of Chien's idea to the $\overline{u_i u_j}$ equations.

An alternative to Eq. (3) has also been suggested by Launder and Reynolds.[23] They derived an asymptotically correct expression for ϵ_{ij} by considering the limiting behavior of ϵ_{ij} as a wall is approached. Their expression, suitably modified by Kebede et al.[24] for periodic pipe flow calculations, can be written as

$$\epsilon_{ij} = \frac{2}{3}\delta_{ij}(1 - f_s)\epsilon + f_s F \frac{\epsilon}{k}\left[\overline{u_i u_j} + \overline{u_i u_k} n_k n_j + \overline{u_j u_k} n_k n_i + \delta_{ij} \overline{u_k u_1} n_k n_1 \right] \tag{4}$$

where $f_s = \exp(-R_t/40)$, $F = (1 + 5\overline{u_2^2}/2k)^{-1}$, $R_t = k^2/\nu\epsilon$, and n_k is the unit vector normal to the wall. The dissipation model, Eq. (4), is quite a bit more complicated than Eq. (3). However, it will be used to close Eq. (1), and the results will be compared with those obtained from Eq. (3).

III. The Governing Equations and Turbulence Closures

For isothermal, incompressible flows, the governing Reynolds equations can be concisely written in Cartesian tensor notation as

$$\frac{\partial U_i}{\partial x_i} = 0 \tag{5}$$

$$U_j \frac{\partial U_i}{\partial x_j} = -\frac{1}{\rho}\frac{\partial P}{\partial x_i} + \frac{\partial}{\partial x_j}\left(\nu \frac{\partial U_i}{\partial x_j} - \overline{u_i u_j} \right) \tag{6}$$

where P is the mean pressure. In writing Eqs. (5) and (6), the assumption of stationary turbulence has been invoked. Closure of Eqs. (5) and (6) is effected by solving them simultaneously with Eq. (1) and a suitable equation for ϵ and assuming appropriate models for D_{ij}^T, Φ_{ij}, and ϵ_{ij}.

Eight low Reynolds number Reynolds-stress closures based on Eqs. (1), (5), and (6) and Chien's[22] modified ϵ equation are examined. The various submodels that are assumed for D_{ij}^T, Φ_{ij}, and ϵ_{ij} are listed in Table 1 and are marked by an x. Their corresponding high Reynolds number versions are designated by a prefix H, such as H-A1, and take on the same models for D_{ij}^T and Φ_{ij}, but with Kolmogorov's[19] isotropic model for ϵ_{ij}. Besides these closures, the low Reynolds number k-ϵ model of Chien,[22] designated by L-k-ϵ, is also used to calculate flows with wall transpiration, and the results are compared with the closures listed in Table 1. Since the same model constants and damping functions as those given by So

and Yoo[25] are used for the present calculations, their values are not quoted here. Interested readers can consult Ref. 25.

The boundary conditions for the elliptic equations (1), (5), and (6) and Chien's ϵ equation include zero gradients in the normal direction at the symmetry axis and in the axial direction at the exit plane. For solid walls, no mass transfer is allowed, and the no-slip condition for all velocity quantities is invoked. In addition, $\epsilon = 0$ at the wall is assumed. When the wall is porous, the mass transfer through the wall is specified.

IV. Method of Solution

For fully developed turbulent flows, the governing equations can be simplified to a set of second-order ordinary differential equations[25] and can easily be solved by the Newton iteration scheme.[26] This is accomplished by normalizing U_i by the friction velocity u_τ, $\overline{u_i u_j}$ by u_τ^2, ϵ by u_τ^3/R, and r by u_τ/ν so that $\eta = u_\tau\ (R-r)/\nu$ is the new dimensionless coordinate for pipe and channel flows and R is the pipe radius or channel half-width. Thus formulated, $Re = u_\tau R/\nu = (u_\tau/2U_0)R_D$ becomes the only input parameter to the fully developed flow calculations,[25] where $R_D = U_0 2R/\nu$ and U_0 is the mean velocity at the pipe or channel center.

A nonuniform grid is used to carry out the calculations. Typically, five grid points are specified between $\eta = 0$ and 5. This is followed by 15 grid points between $\eta = 5$ and 65. The rest of the region $65 \le \eta \le Re$ is then divided into 30–50 grid points, depending on the problem considered. In general, this system of grid spacing is sufficient to give a convergent solution after ~ 1000 iterations, where the weighted residues are $< 10^{-4}$.

For developing flows with or without wall transpiration, the governing equations and boundary conditions are solved numerically using either hybrid or quadratic upwind finite differencing and staggered grids. The iteration sequence employs the SIMPLE algorithm of Patankar and Spalding[27] to solve the momentum equations for a fixed pressure field. After each such sweep over the solution domain, adjustments are made to the pressure field to satisfy continuity along each line of cells. Transport equations for the other quantities are then solved using the calculated velocity field. Iterations are carried out until the momentum and continuity equations are simultaneously satisfied to the required degree of accuracy, usually for relative mass residuals of $\le 1\%$. Again, nonuniform computational grids are used to resolve the flow domain. In the flow direction, 40–60 grid points are used, while the grid spacing worked out in the solution of the ordinary differential equations is used in the normal direction.

In all the developing-flow calculations, besides imposing the exit condition $\partial\psi/\partial x_1 = 0$ where ψ is any flow variable and x_1 is the stream coordinate; another exit condition, $\partial^2\psi/\partial x_1^2 = 0$, has also been tried. The results of these two calculations are essentially the same in the region up to 2 pipe diameters or 2 channel widths from the exit. Therefore, the results presented in this paper are independent of the imposed exit condition.

V. Presentation of Results

Fully developed pipe and channel flows at several Reynolds numbers[14,28–30] are selected for comparison with the model calculations. This is an important first step for the establishment of these closures as both suitable and reliable for near-wall flows. The next step, of course, is to apply the closures to a more complex flowfield, as in the uniform suction experiment of Weissberg.[12] Once verified, the validity of the low Reynolds number closures for near-wall flows with and without wall transpiration is established.

The input parameter for the fully developed flow calculations is Re. Its value is 1052 for Lanfer's[14] experiment, 489 for Schildknecht et al.'s[28] experiment, and 626, 738, and 1463 for the three sets of measurements from Refs. 29 and 30. The model constants used for these calculations are given in Ref. 25. The pipe flow results for models A1, A2, B1, and B2 are shown in Figs. 1a and 2–5, while those for models A3 and B3 are plotted in Figs. 1b and 6. Since the results for models C1 and C2 are essentially identical to those given by models A1 and B2, respectively, they are not shown in the figures. Finally, the channel flow results are given in Figs. 7–9 and the uniform suction flow results are plotted in Figs. 10–12. For the sake of clarity, the results are summarized in the following sections.

A. Effects of Dissipation Modeling

In general, both dissipation models (A2, C1 or B2, C2) give reasonably good results for U, $\overline{uv}$, k, and ϵ (see Figs. 1a and 2–4). However, they fail to replicate correctly the behavior of the normal stresses ($\overline{u^2}$, $\overline{v^2}$, and $\overline{w^2}$) near the wall (see Fig. 5). The calculated U is in good agreement with measurements in the near-wall region but shows a substantial discrepancy in the pipe core (see Fig. 1a), even though the logarithmic behavior in this region is recovered. The measured U can be correlated by a logarithmic law of the wall such that

$$U/u_\tau = A\,\ell n\,\eta + B \tag{7}$$

where $A = \ell/\kappa$, κ is the von Kármán constant and B is parametically dependent on R_D.[31] For the pipe flow experiments,[14,28] the constants thus determined are listed in Table 2 together with the quantity U_0/u_τ. Likewise, these quantities can also be determined from the model calculations. They are also listed in Table 2 for comparison. It can be seen that the measured slope of the log-law is not in agreement with the calculated slopes and the calculated U_0/u_τ are always lower than the measured values.

In order to understand the discrepancy noted between the measured and calculated U, the U obtained by integrating the mean flow equations using the measured $\overline{uv}$ as input is also shown in Fig. 1a for comparison with the model calculations. The corresponding A, B, and U_0/u_τ are listed in Table 2. It can be seen that the U thus determined is in excellent agreement with the calculated U profiles. This shows that the measured U and $\overline{uv}$ are not quite consistent, and the compari-

Table 1 The labeling of different turbulence closures

	Diffusion model for D_{ij}^T			Redistribution model for Φ_{ij}		Dissipation model for ϵ_{ij}	
Closure	Ref. 2	Ref. 18	Ref. 17	Ref. 7 without wall correction	Ref. 7 with wall correction	Eq. (3)	Eq. (4)
A1	×		×			×	
A2	×			×		×	
A3	×				×	×	
B1		×	×			×	
B2		×		×		×	
B3		×			×	×	
C1	×			×			×
C2		×		×			×

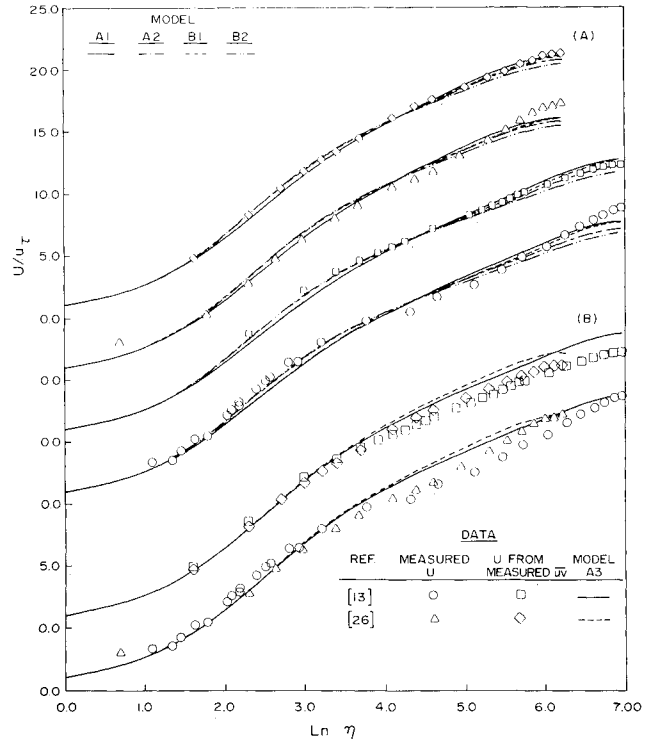

Fig. 1 Comparison of calculated and measured U plotted in wall coordinates for fully developed pipe flows.

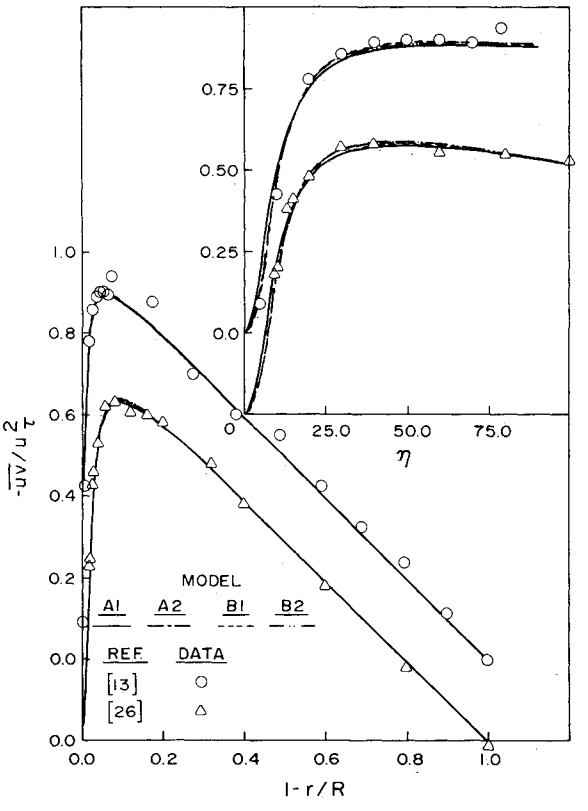

Fig. 2 Comparison of calculated and measured $\overline{uv}$ for fully developed pipe flows.

Table 2 Comparison of the calculated and measured constants in the logarithmic law of the wall

		Laufer[14]			Schildknecht et al.[28]		
		A (κ)	B	U_0/U_τ	A (κ)	B	U_0/u_τ
	Measured U	2.50 (0.40)	5.2	23.76	2.50 (0.40)	5.45	22.25
Closure	U from measured $\overline{uv}$	2.60 (0.38)	5.00	22.29	2.53 (0.40)	5.90	21.23
A1		2.65 (0.38)	5.00	22.69	2.66 (0.38)	5.31	21.08
A2		2.46 (0.41)	5.69	22.10	2.48 (0.40)	6.00	20.79
A3		2.66 (0.38)	5.96	23.79	2.91 (0.34)	5.01	22.26
B1		2.62 (0.38)	5.00	22.60	2.69 (0.37)	5.00	20.79
B2		2.35 (0.43)	6.10	21.70	2.45 (0.41)	5.95	20.43
B3		2.34 (0.43)	7.04	22.70	2.43 (0.41)	6.91	21.33
C1		2.51 (0.40)	6.09	22.86	2.74 (0.37)	5.37	21.60
C2		2.23 (0.45)	6.64	21.59	2.32 (0.43)	6.55	20.36

sons shown in Figs. 1a and 2–5 can be considered excellent. However, models C1 and C2 consistently predict the wrong behavior for B as R_D is decreased. Models A2 and B2 give the right trend while models C1 and C2 do not. In spite of this, the two dissipation models, Eqs. (3) and (4), give realistic results and can predict near-wall flow behavior very well.

B. Effects of Mean-Strain Modeling

As far as U, $\overline{uv}$, k, and ϵ predictions are concerned, the simple return-to-isotropy model (A1 or B1) is just as promising as the more complete model of Launder et al.[7] (A2 or B2), at least for fully developed pipe flow calculations. However, one advantage of Launder et al.'s model is its ability to predict different levels for $\overline{v^2}$ and $\overline{w^2}$, which are more realistic. Otherwise, both models suffer the same shortcomings—namely, the underestimation of the rise of $\overline{u^2}$ and the overestimation of the increase of $\overline{v^2}$ and $\overline{w^2}$ near the wall (see Fig. 5). Also, they fail to predict the isotropic behavior of the turbulence field at the pipe center. As a result, k distribution in the pipe center is overpredicted.

C. Effects of Diffusion Modeling

The comparison should now be made between models A1, A2 and B1, B2. It can be seen that model B2 still gives rise to the underprediction of A and U_0/u_τ and the overestimation of B. The parametric dependence of B on R_D is incorrectly predicted. Instead of predicting an increase for B as R_D decreases, it gives a B that decreases slightly with R_D. On the other hand, model B1 gives essentially the same values for A and U_0/u_τ but a constant B. In view of these incorrect trends, it can be concluded that the performance of B1 and B2 does not fair well with A1 and A2.

The near-wall behaviors of U, $\overline{uv}$, k, and ϵ are again well predicted. This shows that the model flow near a wall is essentially governed by the dissipation model and is only slightly dependent on the diffusion and redistribution models. Therefore, the calculations indicate that once a gradient diffusion model is assumed, the results are only slightly dependent on the behavior of the turbulent diffusivity and redistribution model. A return-to-isotropy model will give results that are quite similar to those obtained from Launder et al.'s model. Also, there is a little difference between an isotropic and a nonisotropic model for turbulent diffusion.

D. Effects of Wall Correction on Redistribution Modeling

Since the presence of a rigid wall affects the pressure field, thus impeding the transfer of turbulence energy from the streamwise direction to that normal to the wall, Launder

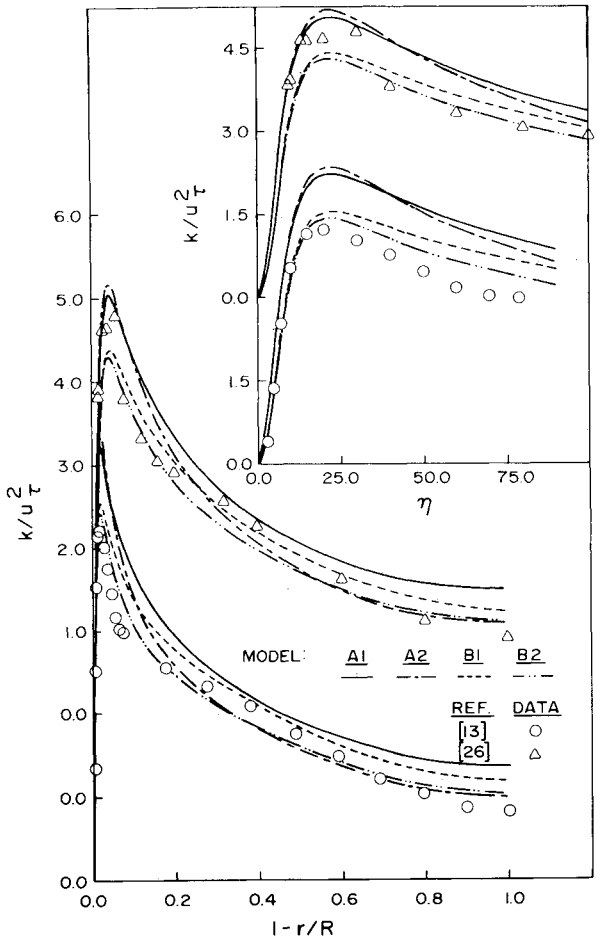

Fig. 3 Comparison of calculated and measured k for fully developed pipe flows.

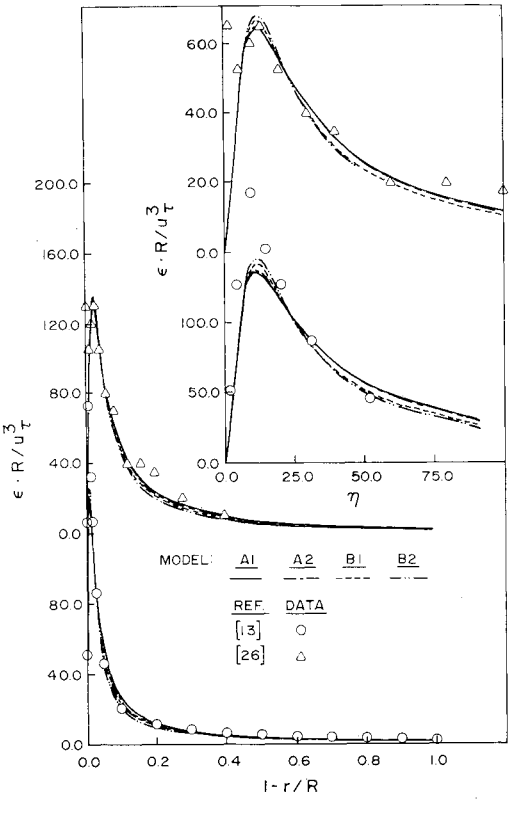

Fig. 4 Comparison of calculated and measured ϵ for fully developed pipe flows.

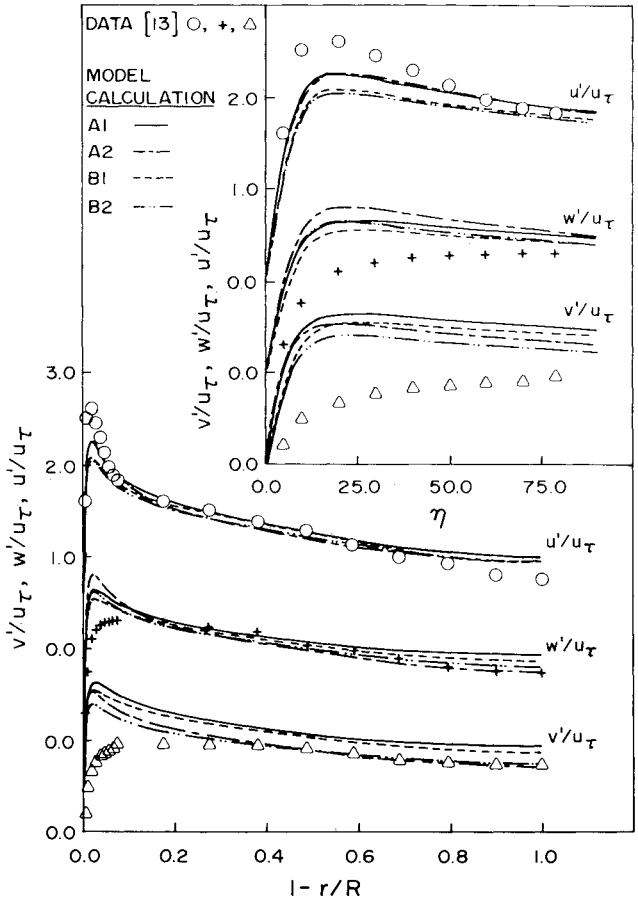

Fig. 5 Comparison of calculated and measured normal stresses for fully developed pipe flows.

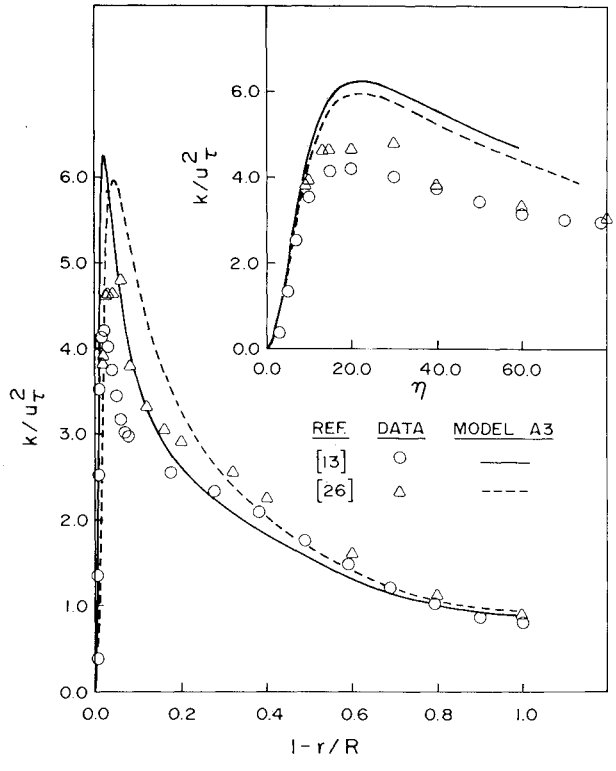

Fig. 6 Comparison of calculated and measured k to illustrate effects of wall correction.

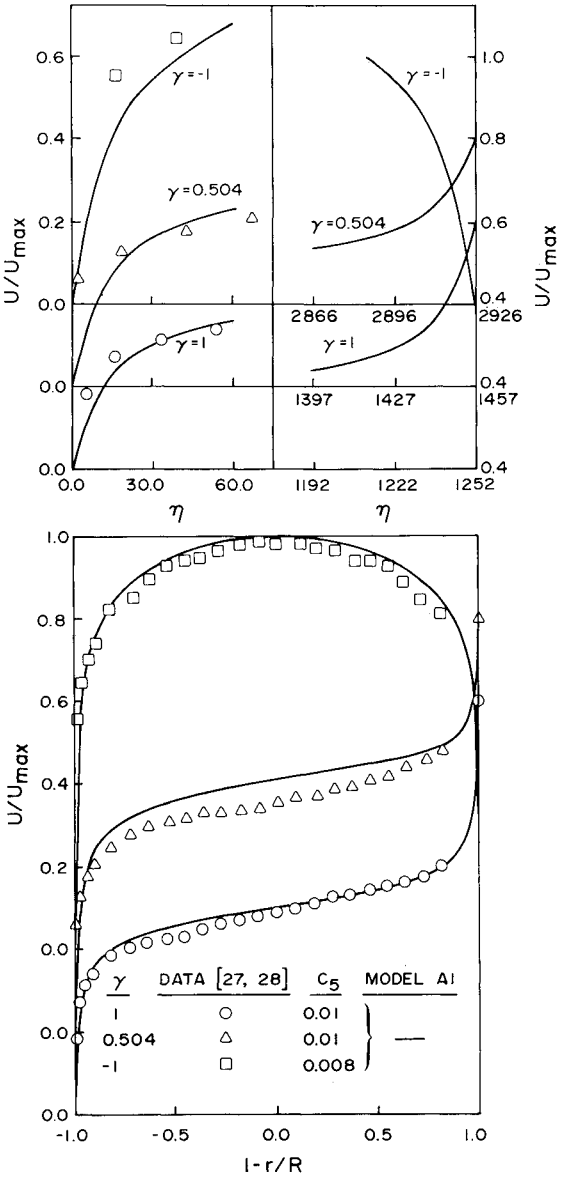

Fig. 7 Comparison of calculated and measured U for channel flows.

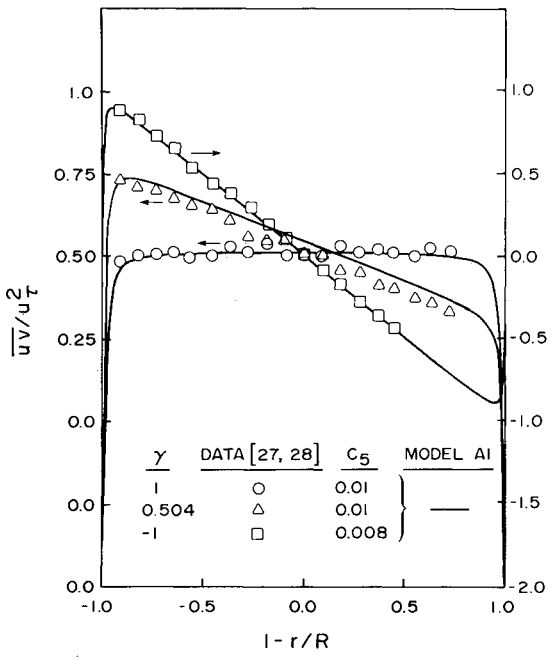

Fig. 8 Comparison of calculated and measured $\overline{uv}$ for channel flows.

et al.[7] propose a wall correction to the redistribution model to account for this wall effect. The correction is designed specifically to model the decrease of the turbulence energy transfer to the normal direction. Since then, wall correction has been used by Irwin and Smith[6] to model curved-shear flows and by Gibson and Launder[20] to model atmospheric boundary layers. However, in these calculations, the near-wall flow is not resolved directly. Therefore, the value of wall correction in redistribution modeling has not been clearly demonstrated. The present approach allows the near-wall flow to be calculated directly and thus provides a good opportunity to assess the relative merits of wall correction.

To do this, the modeled equations are solved with the wall correction terms included, i.e., model A3 is used to calculate the fully developed pipe flows. In the course of solving these equations, it is found that if C_{1w} and C_{2w} are used, as suggested by Launder et al., convergent solutions to the governing equations are not possible. The problem is traced to the coefficients of the terms $(\overline{u_i u_i} - 2k/3)$ in the three Reynolds normal stress equations. After normalization, the coefficients become $[C_1/Re - C_{1w}(k/u_\tau^2)^{3/2}\epsilon R\eta/u_\tau^3]$. If $C_{1w} = 0.125$ is used, as suggested by Launder et al., the coefficient becomes negative over a substantial portion of the pipe. Consequently, these terms $(\overline{u_i u_i} - 2k/3)$ change sign and the equations are not balanced. A similar behavior is also observed in the production term in the Reynolds shear stress equation because C_{2w} is too large. Subsequently, C_{1w} and C_{2w} are slowly decreased until convergent solutions to the modeled equations are obtained. The values of C_{1w} and C_{2w} thus determined are 0.0625 and 0.0075 respectively. Two sets of model calculations are performed, carried out with models A3 and B3. The calculated A, B, and U_0/u_τ are listed in Table 2 for comparison.

Only the A3 model results for U and k are shown in Figs. 1b and 6, while the B3 model results for A, B, and U_0/u_τ are also listed in Table 2 for comparison. They serve to illustrate the differences between these results and those shown in Figs. 1a and 2–5. In general, wall correction increases A, B, U_0/u_τ, and the peak value of k. Therefore, the disagreement between the measurements and the predictions becomes worse. With the quoted values of C_{1w} and C_{2w}, the peak value of k is more than 20% higher than the measured data. Calculations are also performed with $C_{1w} = 0.05$ and $C_{2w} = 0.006$. The results are essentially similar to those shown in Figs. 1b and 6. However, the A, B, and U_0/u_τ values are slightly smaller than those shown in Table 2, and the peak value of k is reduced to ~ 8% higher than the measured data. Further reduction of C_{1w} and C_{2w} to 0.025 and 0.003, respectively, gives results that are essentially identical to those shown in Figs. 1a and 2–5, and the discrepancy noted in the k prediction disappears. This shows that wall correction with small values specified for the constants C_{1w} and C_{2w} essentially has no effect on the calculations. Therefore, wall correction as suggested by Launder et al.[7] is inappropriate.

E. Channel Flow Calculations

A thorough examination of the different closures on near-wall flow calculations has been carried out in Secs. A–D for fully developed pipe flows. The A1 model emerges as the most promising because of its simplicity and accurate predictions of near-wall flows. The further validation of this model together with A2, B1, and B2 is carried out with other types of fully developed turbulent flows. The data are drawn from the pure Couette flow ($\gamma = 1$), pure Poiseuille flow ($\gamma = -1$), and combined Couette/Poiseuille flow ($\gamma = 0.504$) measurements of

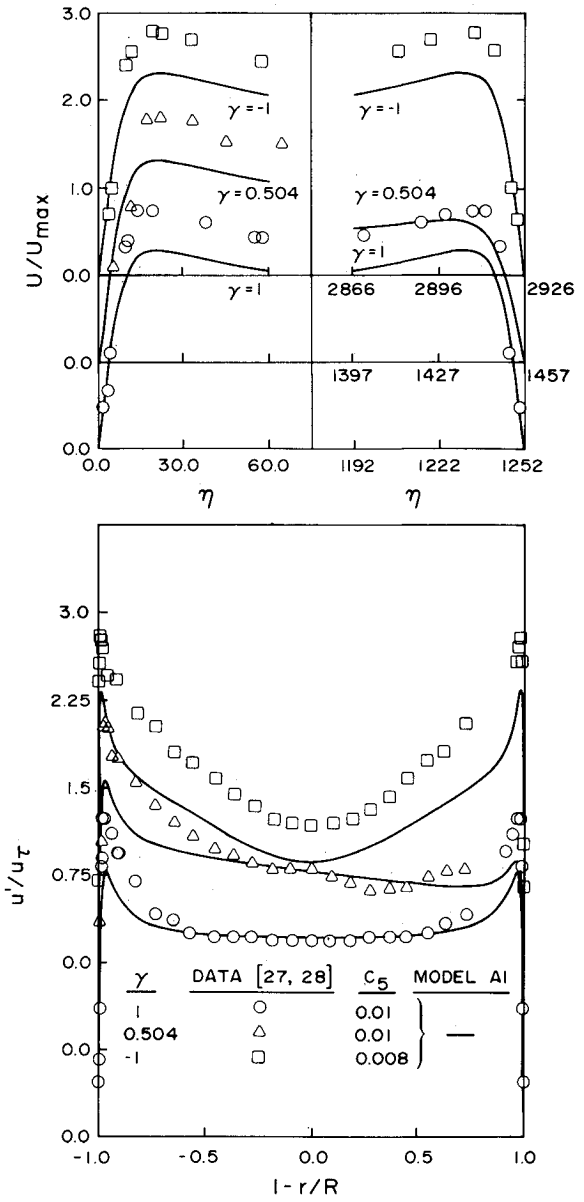

Fig. 9 Comparison of calculated and measured u' for channel flows.

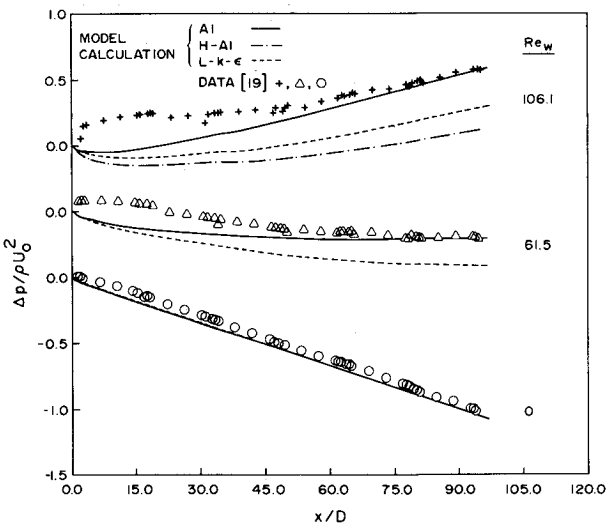

Fig. 10 Comparison of measured and calculated axial pressure drop along pipes with and without uniform wall suction.

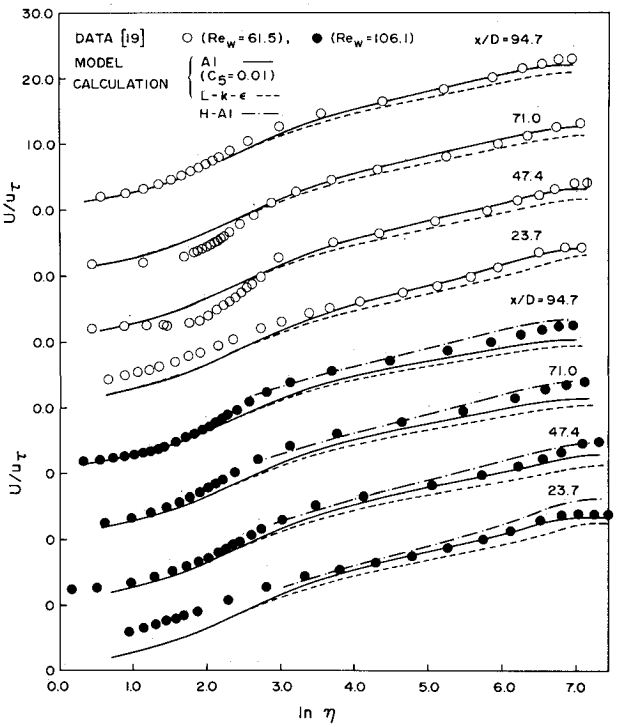

Fig. 11 Comparison of measured and calculated U for the cases of $Re_w = 61.5$ and 106.1.

El Telbany and Reynolds,[29,30] where γ is the ratio of the stresses at the two walls. Thus, the low Reynolds number closures are also tested against flows with a moving wall. The comparisons for U, $\overline{uw}$, and $u' = \sqrt{\overline{u^2}}$ are shown in Figs. 7–9. Only the results of A1 are plotted because the other calculations are practically identical to those shown in Figs. 7–9. In these figures, U_{max} is the maximum U velocity in the channel, and the values of C_5 used to carry out the calculations are also listed in the figures. Otherwise, all the model constants used are as given in Ref. 25.

As expected, the model calculations are in excellent agreement with the measurements for U and $\overline{uw}$. Again, u' are not predicted correctly. The rise of u' near the wall, whether stationary or moving, is underpredicted, just as in the pipe flow case. Perhaps the reason is the inability of the redistribution model to mimic the energy transfer from the stream direction to that normal to the wall. It could also be due to the fact that the dissipation model is dissipating too much turbulence energy near the wall, thus leading to lower values for the turbulent normal stresses. Similar results for u' are given by A2; however, A2 gives different levels for $\overline{v^2}$ and $\overline{w^2}$ while A1 predicts the same level for these two normal stresses. Other than this one advantage, A2 predictions are essentially the same as A1. In general, the channel flow comparisons reveal the same shortcomings as the pipe flow comparisons using models A1, A2, B1, and B2. Therefore, A1 is the model of choice for complex wall shear flow calculations because of its simplicity.

F. Effects of Uniform Wall Suction

The uniform wall suction calculations are carried out for the experiments of Weissberg.[12] Three cases are selected for comparison: 1) $Re_w = 0$, 2) $Re_w = 61.5$, and 3) $Re_w = 106.1$, where $Re_w = v_w D/\nu$, v_w is the uniform suction velocity and D the pipe diameter. All three cases have an exit Reynolds number, $Re_0 = U_0 D/\nu$ where U_0 is the average exit pipe velocity, of 39,800. The inlet Reynolds number, $Re_i = U_i D/\nu$ where U_i is the average inlet pipe velocity, is 39,800, 63,100, and 80,000, respectively, for cases 1–3. The pipe diameter is

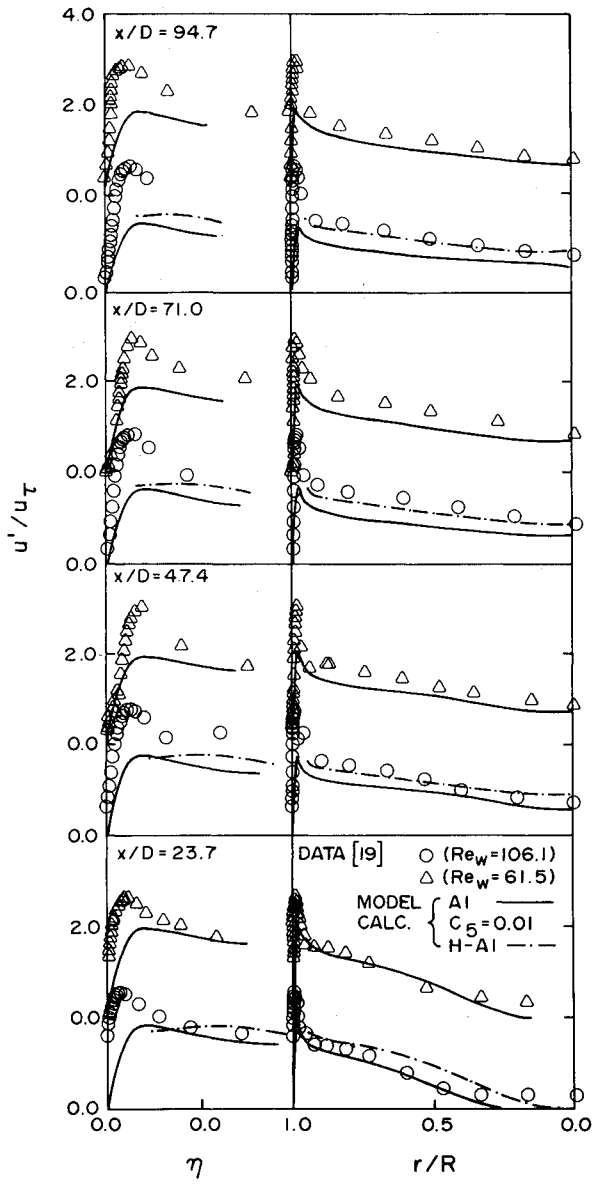

Fig. 12 Comparison of measured and calculated u' for the cases of $Re_w = 61.5$ and 106.1.

$D \simeq 77$ mm, the mean entrance conditions are as specified by Weissberg,[12] and the turbulence conditions at inlet are deduced from the local equilibrium assumption. Once determined, these conditions are used for all model calculations. Only the L-k-ϵ and A1 model results are compared in detail with measurements because conventional wall functions are known to be inadequate for flows with wall transpiration. However, the inadequacy of wall functions is illustrated by the comparison of H-A1 model calculations with those of A1 and L-k-ϵ for the case of $Re_w = 106.1$ only. The comparisons are shown in Figs. 10–12, where the value of C_5 used for each case is also specified. Other than this one change, the model constants given in Ref. 25 are kept for the model calculations. Since the measurements on axial pressure drop, Δp, $U(r)$, and $u'(r)$ are available, comparisons are made with these data only.

Since L-k-ϵ and A1 give essentially the same predictions for Δp and U for case 1, the L-k-ϵ calculations are not shown in Fig. 10. There is no prediction of u' due to L-k-ϵ, so in Fig. 12 only the results of H-A1 and A1 are shown. Also, the results show that the developing pipe flow with zero wall suction is correctly predicted by both L-k-ϵ and A1. Therefore, the U results for case 1 are not shown in Fig. 11. As discussed earlier, A1 again fails to predict correctly the rise of u' near the wall. In spite of this, u' distributions across the pipe in the stream direction are very well reproduced by model A1. The performance of L-k-ϵ starts to deteriorate when uniform suction is present in the pipe flow (see Figs. 10–12). Since mass is continuously being removed, a true fully developed pipe flow condition is not possible when $Re_w > 0$. However, the exit boundary condition, $\partial\psi/\partial x = 0$ or $\partial^2\psi/\partial x^2 = 0$, gives essentially the same results for the region shown in the figures. Therefore, the results presented are independent of the exit boundary condition. The results of H-A1 are also shown in Figs. 10–12 for comparison with the calculations of L-k-ϵ and A1. This comparison clearly shows the inadequacy of H-A1 for flows with uniform wall suction. Agreement between the H-A1 predictions and the measurements of Δp deteriorates as Re_w increases. On the other hand, the good agreement shown in U/u_τ (see Fig. 11) between H-A1 and the measurements is a consequence of the incorrect prediction of u_τ. Therefore, the question "Time to abandon wall functions?" posed by Launder[32] should be answered in the affirmative. In general, L-k-ϵ overpredicts the axial pressure drop in the presence of a nonzero Re_w (see Fig. 10). It underestimates the mean velocity in the region away from the wall (see Fig. 11). However, its prediction of the near-wall flow is just as good as that of A1. Again, the rise of u' near the wall is incorrectly calculated by A1 (see Fig. 12). The extent of the discrepancy is about the same as that noted for the zero-suction case. Consequently, it can be concluded that, among all the closures considered, A1 gives the best predictions of developing pipe flows with a uniform suction.

VI. Conclusions

A low Reynolds number turbulence closure for the full set of Reynolds-stress equations is proposed. The proposal is based on a gradient diffusion model for turbulent diffusion, a conventional high Reynolds number model for redistribution, and a modified dissipation model that accounts for viscous effects near a wall. Validation of the closure is carried out with fully developed turbulent flows at several Reynolds numbers and a developing pipe flow with a uniform wall suction. In general, the closure gives good results for U, $\overline{uv}$, k, and ϵ but fails to reproduce the behavior of the normal turbulent stresses near a wall. These discrepancies cannot be erased by modifying the redistribution model to account for the reduced turbulence energy transfer from the streamwise direction to that normal to a wall, as suggested by Launder et al.[7] Neither can the correlations between the predictions and the measurements be improved by the inclusion of mean-strain terms in the modeling of the redistribution term. Furthermore, it is found that once the gradient diffusion assumption is invoked, the calculated results are only slightly dependent on the assumed behavior of the turbulent diffusivity.

All the Reynolds-stress closures examined show the same shortcomings when applied to the calculation of turbulent flows with and without wall transpiration. They fail to predict the steep rise of the normal stresses near a wall and the isotropic behavior of the turbulence field at the pipe center. However, model A1 is fairly simple and seems to provide an accurate and realistic prediction of the mean flow and turbulence intensities near a wall. In view of this, it can be concluded that A1 is best suited for turbulent flow calculations with and without wall transpiration.

Acknowledgments

This research was supported by NASA Grant NAG 3-167, monitored by J.D. Holdeman, and by Naval Weapons Center, China Lake, CA, under Contract N60530-85-C-0191, monitored by F. Zarlingo. The first author further acknowledges support from Oak Ridge National Laboratory, Oak Ridge, TN, under Subcontract 11X-57502V.

References

[1]Hanjalic, K. and Launder, B.E., "A Reynolds-stress Model of Turbulence and its Application to Thin Shear Flows," *Journal of Fluid Mechanics*, Vol. 52, 1972, pp. 609–638.

[2]Hanjalic, K. and Launder, B.E., "Contribution Towards a Reynolds-stress Closure for Low-Reynolds-Number Turbulence," *Journal of Fluid Mechanics*, Vol. 74, 1976, pp. 593–610.

[3]Launder, B.E., Morse, A., Rodi, W., and Spalding, D.B., "Prediction of Free Shear Flows—A Comparison of the Performance of Six Turbulence Models," NASA SP-321, 1972, pp. 361–426.

[4]Mellor, G.L. and Herring, H.J., "A Survey of the Mean Turbulent Field Closure Models," *AIAA Journal*, Vol. 11, May 1973, pp. 590–599.

[5]Mellor, G.L. and Yamada, T., "A Hierarchy of Turbulence Closure Models for Planetary Boundary Layers," *Journal of Atmospheric Science*, Vol. 31, 1974, pp. 1791–1806.

[6]Irwin, H.P.A.H. and Smith, P.A., "Prediction of the Effect of Streamline Curvature on Turbulence," *Physics of Fluids*, Vol. 18, 1975, pp. 624–630.

[7]Launder, B.E., Reece, G.J., and Rodi, W., "Progress in the Development of a Reynolds-Stress Turbulence Closure," *Journal of Fluid Mechanics*, Vol. 68, 1975, pp. 537–566.

[8]Gibson, M.M. and Rodi, W., "A Reynolds-stress Closure Model of Turbulence Applied to the Calculation of a Highly Curved Mixing Layer," *Journal of Fluid Mechanics*, Vol. 103, 1981, pp. 161–182.

[9]Stratford, B.S., "An Experimental Flow with Zero Skin Friction Throughout its Region of Pressure Rise," *Journal of Fluid Mechanics*, Vol. 5, 1959, pp. 17–35.

[10]Jones, W.P. and Launder, B.E., "Some Properties of Sink-Flow Turbulent Boundary Layers," *Journal of Fluid Mechanics*, Vol. 56, 1972, pp. 337–351.

[11]Bissonnette, L. and Mellor, G.L., "Experiments on the Behavior of an Axisymmetric Turbulent Boundary Layer with a Sudden Circumferential Strain," *Journal of Fluid Mechanics*, Vol. 63, 1974, pp. 369–413.

[12]Weissberg, H.L., "Velocity and Pressure Distributions in Turbulent Pipe Flow with Uniform Wall Suction," Ph.D. Thesis, University of Tennessee, Knoxville, 1954.

[13]Jones, W.P. and Launder, B.E., "The Prediction of Laminarization with a Two-equation Model of Turbulence," *International Journal of Heat and Mass Transfer*, Vol. 15, 1972, pp. 301–314.

[14]Laufer, J., "The Structure of Turbulence in Fully-Developed Pipe Flow," NACA Rept. 1174, 1954.

[15]Eckelman, H., "Experimentelle Untersuchungen in einer turbulumten Kanalstromung mit starken viskosen Wandochichten," *Mitt. Max-Planck Inst. f. Stromungsforschung*, Gottingen, 48, 1970.

[16]Patel, V.C. and Head, M.C., "Some Observations of Skin Friction and Velocity Profiles in Fully Developed Pipe and Channel Flows," *Journal of Fluid Mechanics*, Vol. 38, 1969, pp. 181–201.

[17]Rotta, J.C., "Statistische Theorie Nichthomogener Turbulenz," *Zeit. fur Physik*, Vol. 129, 1951, pp. 547–572; Vol. 131, 1951, pp. 51–77.

[18]Daly, B.J. and Harlow, F.H., "Transport Equations of Turbulence," *Physics of Fluids*, Vol. 13, 1970, pp. 2634–2649.

[19]Kolmogorov, A.N., "The Local Structure of Turbulence in Incompressible Viscous Fluid for Very Large Reynolds Numbers," Compt. rend. acad. sci. U.R.S.S., Vol. 30, 1941, pp. 301–305.

[20]Gibson, M.M. and Launder, B.E., Ground Effects on Pressure Fluctuations in the Atmospheric Boundary Layer," *Journal of Fluid Mechanics*, Vol. 86, 1978, pp. 491–511.

[21]Hinze, J.O., *Turbulence*, McGraw-Hill, New York, 1959.

[22]Chien, K.Y., "Predictions of Channel and Boundary Layer Flows with a Low-Reynolds-Number Two-equation Model of Turbulence," *AIAA Journal*, Vol. 20, Jan. 1982, pp. 33–38.

[23]Launder, B.E. and Reynolds, W.C., "Asymptotic Near-Wall Stress Dissipation Rates in a Turbulent Flow," *Physics of Fluids*, Vol. 26, 1983, pp. 1157–1158.

[24]Kebede, W., Launder, B.E., and Younis, B.A., "Large Amplitude Periodic Pipe Flow: A Second-Moment Closure Study," *Proceedings of the 5th Turbulent Shear Flows Symposium*, Ithaca, New York, 1985, pp. 16 · 23–16 · 29.

[25]So, R.M.C. and Yoo, G.J., "On the Modelling of Low-Reynolds-Number Turbulence," NASA CR-3994, 1986.

[26]Na, T.Y., *Computational Methods in Engineering Boundary Value Problems*, Academic Press, New York, 1979.

[27]Patankar, S.V. and Spalding, D.B., "A Calculation Procedure for Heat, Mass and Momentum Transfer in Three-Dimensional Parabolic Flows," *International Journal of Heat and Mass Transfer*, Vol. 15, 1972, pp. 1787–1806.

[28]Schildknecht, M., Miller, J.A., and Meier, G.E.A., "The Influence of Suction on the Structure of Turbulence in Fully-Developed Pipe Flow," *Journal of Fluid Mechanics*, Vol. 90, 1979, pp. 67–107.

[29]El Telbany, M.M.M. and Reynolds, A.J., "Velocity Distributions in Plane Turbulent Channel Flows," *Journal of Fluid Mechanics*, Vol. 100, 1980, pp. 1–29.

[30]El Telbany, M.M.M. and Reynolds, A.J., "Turbulence in Plane Channel Flows," *Journal of Fluid Mechanics*, Vol. 111, 1981, pp. 283–318.

[31]Afzal, N. and Yajnik, K., "Analysis of Turbulent Pipe and Channel Flows at Moderately Large Reynolds Number," *Journal of Fluid Mechanics*, Vol. 61, 1973, pp. 23–31.

[32]Launder, B.E., "Numerical Computation of Convective Heat Transfer in Complex Turbulent Flows: Time to Abandon Wall Functions?" *International Journal of Heat and Mass Transfer*, Vol. 27, 1984, pp. 1485–1491.